

Published in final edited form as:

Circ Res. 2008 August 1; 103(3): 279–288. doi:10.1161/CIRCRESAHA.108.175919.

Enhancing Mitochondrial Ca²⁺ Uptake in Myocytes From Failing Hearts Restores Energy Supply and Demand Matching

Ting Liu and Brian O'Rourke

From the Division of Cardiology, The Johns Hopkins University, Baltimore, Md.

Abstract

Mitochondrial ATP production is continually adjusted to energy demand through coordinated increases in oxidative phosphorylation and NADH production mediated by mitochondrial Ca²⁺ ([Ca²⁺]_m). Elevated cytosolic Na⁺ impairs [Ca²⁺]_m accumulation during rapid pacing of myocytes, resulting in a decrease in NADH/NAD⁺ redox potential. Here, we determined 1) if accentuating [Ca²⁺]_m accumulation prevents the impaired NADH response at high [Na⁺]_i; 2) if [Ca²⁺]_m handling and NADH/NAD⁺ balance during stimulation is impaired with heart failure (induced by aortic constriction); and 3) if inhibiting [Ca²⁺]_m efflux improves NADH/NAD⁺ balance in heart failure. [Ca²⁺]_m and NADH were recorded in cells at rest and during voltage clamp stimulation (4Hz) with either 5 or 15 mmol/L [Na⁺]_i. Fast [Ca²⁺]_m transients and a rise in diastolic [Ca²⁺]_m were observed during electric stimulation. [Ca²⁺]_m accumulation was [Na⁺]_i-dependent; less [Ca²⁺]_m accumulated in cells with 15 Na⁺ versus 5 mmol/L Na⁺ and NADH oxidation was evident at 15 mmol/L Na⁺, but not at 5 mmol/L Na⁺. Treatment with either the mitochondrial Na⁺/Ca²⁺ exchange inhibitor CGP-37157 (1 μmol/L) or raising cytosolic P_i (2 mmol/L) enhanced [Ca²⁺]_m accumulation and prevented the NADH oxidation at 15 mmol/L [Na⁺]_i. In heart failure myocytes, resting [Na⁺]_i increased from 5.2±1.4 to 16.8±3.1 mmol/L and net NADH oxidation was observed during pacing, whereas NADH was well matched in controls. Treatment with CGP-37157 or lowering [Na⁺]_i prevented the impaired NADH response in heart failure. We conclude that high [Na⁺]_i (at levels observed in heart failure) has detrimental effects on mitochondrial bioenergetics, and this impairment can be prevented by inhibiting the mitochondrial Na⁺/Ca²⁺ exchanger.

Keywords

energy metabolism; excitation–contraction coupling; heart failure; ion transport; Na⁺/Ca²⁺ exchanger; oxidative phosphorylation

Cardiac muscle contraction requires continuous matching of ATP supply with a constantly varying workload, yet the mechanism of mitochondrial bioenergetic control is still incompletely understood. The rate of oxidative phosphorylation depends on the protonmotive force across the inner membrane, which is influenced by the balance between the rate of production of reducing equivalents (NADH and FADH₂) by the tricarboxylic acid (TCA) cycle and the rate of electron transfer to O₂ by the respiratory chain. When energy demand increases,

© 2008 American Heart Association, Inc.

Correspondence to Brian O'Rourke, PhD, The Johns Hopkins University, Institute of Molecular Cardiobiology, 720 Rutland Avenue, 1059 Ross Building, Baltimore, MD 21205-2195. E-mail E-mail: bor@jhmi.edu.

Reprints: Information about reprints can be found online at <http://www.lww.com/reprints>

This manuscript was sent to Hans Michael Piper, Consulting Editor, for review by expert referees, editorial decision, and final disposition.

Disclosures

None.

NADH oxidation is accelerated, requiring a concomitant increase in dehydrogenase activity to maintain NADH/NAD⁺ redox potential and ATP production. Two main lines of evidence support the idea that mitochondrial Ca²⁺ ([Ca²⁺]_m) homeostasis plays a central role in energy supply and demand matching. First, matrix-free Ca²⁺ activates several enzymes in the TCA cycle, including pyruvate dehydrogenase, 2-oxoglutarate dehydrogenase, and NAD⁺-linked isocitrate dehydrogenase,¹ thereby increasing NADH production. Second, increases in [Ca²⁺]_m have been recorded during excitation–contraction coupling and are correlated with changes in metabolism, indicating that mitochondria take up Ca²⁺ in response to cytosolic Ca²⁺ on a beat-to-beat basis (reviewed in ^{2,3}). The mitochondrial Ca²⁺ uniporter and the mitochondrial Na⁺/Ca²⁺ exchanger (mNCE) are the major pathways for Ca²⁺ transport across the cardiac mitochondrial inner membrane.⁴ Mitochondrial Ca²⁺ uniporter transports Ca²⁺ down its electrochemical gradient into the matrix, whereas mNCE extrudes Ca²⁺ from mitochondrial matrix in exchange for Na⁺. The kinetics of the 2 pathways are different; Ca²⁺ uptake can occur rapidly during the cytosolic Ca²⁺ ([Ca²⁺]_c) transient, but [Ca²⁺]_m decay kinetics are slow, leading to [Ca²⁺]_m accumulation in response to an increase in stimulation frequency or Ca²⁺ transient amplitude.⁵ It is hypothesized that the accumulation of [Ca²⁺]_m is critical for matching NADH redox potential and ATP production to increased energetic demand. Thus, interruption of [Ca²⁺]_m accumulation should have an impact on cardiac mitochondrial energetics in response to increased work.

The [Na⁺]_i dependence of [Ca²⁺]_m efflux and its effect on NADH during increased work in normal myocytes has led us to propose that the mitochondrial energetic response might be altered in cardiac pathologies in which [Na⁺]_i is elevated, including models of cardiac hypertrophy and failure.^{3,5} High [Na⁺]_i in heart failure has been studied in relation to its effects on Ca²⁺ handling and contraction, and it is well established that elevated [Na⁺]_i has an inotropic effect by altering the driving force for the forward and reverse modes of the sarcolemmal Na⁺/Ca²⁺ exchanger.^{6–8} However, there have been very few studies on the effects of elevated [Na⁺]_i on mitochondrial Ca²⁺ uptake and bioenergetics.^{5,9,10}

In the present study, we investigate whether accentuating [Ca²⁺]_m accumulation, by inhibiting the mNCE or by increasing cytosolic inorganic phosphate (P_i), abrogates the effects of high [Na⁺]_i on the NADH response. Moreover, we demonstrate that elevated [Na⁺]_i impairs NADH production during rapid stimulation in cardiomyocytes from failing hearts and that this defect can be reversed by mNCE inhibition or lowering [Na⁺]_i to improve the mitochondrial redox balance in heart failure.

Materials and Methods

An expanded methods section is included in the online data supplement available at <http://circres.ahajournals.org>. Briefly, isolated guinea pig cardiomyocytes were subjected to rapid change of workload: from resting state to 4-Hz stimulation and then back to resting state in the presence of 100 nmol/L isoproterenol. NADH autofluorescence was recorded. [Ca²⁺]_m was monitored with rhod-2 and [Na⁺]_i was measured with SBFI. The heart failure model was produced with ascending aortic constriction.

Results

[Na⁺]_i Effect on Mitochondrial Ca²⁺ Accumulation and NADH Production During Increased Workload

NADH autofluorescence and [Ca²⁺]_m were recorded in patch-clamped cells (to eliminate cytosolic rhod-2) with either 5 or 15 mmol/L Na⁺ in the pipette solution as previously described.⁵ Rhod-2 fluorescence intensity increased during stimulation in both the 5 and 15 mmol/L [Na⁺]_i groups (Figure 1A–B); however, [Ca²⁺]_m accumulation was attenuated by 15 mmol/L

$[\text{Na}^+]_i$. The amplitude of the $[\text{Ca}^{2+}]_m$ transient was decreased by approximately 40% compared with cells with 5 mmol/L $[\text{Na}^+]_i$ (Figure 1B). Diastolic normalized rhod-2 fluorescence (F/F0) was 1.21 ± 0.041 in 15 mmol/L $[\text{Na}^+]_i$ at the end of stimulation and 1.07 ± 0.04 after 100-second recovery at rest (Figure 1B), whereas with 5 mmol/L $[\text{Na}^+]_i$, it was 1.35 ± 0.05 at the end of stimulation and 1.16 ± 0.04 after 100-second recovery at rest (Figure 1A). The decrease of $[\text{Ca}^{2+}]_m$ accumulation in the cells with 15 mmol/L Na^+ was associated with net oxidation of NADH. On a rapid increase of workload (4 Hz stimulation for 100 seconds) from rest with 15 mmol/L Na^+ , NADH gradually decreased from $82.1 \pm 4.1\%$ before stimulation to $63.7 \pm 7.4\%$ at the end of stimulation (Figure 1D). In contrast, with 5 mmol/L Na^+ , the NADH levels were maintained during stimulation: NADH was $67.7 \pm 5.8\%$ before stimulation and $66.3 \pm 6.3\%$ at the end of stimulation (Figure 1C).

Effects of the Mitochondrial $\text{Na}^+/\text{Ca}^{2+}$ Exchanger Inhibitor CGP-37157

To investigate whether restoration of $[\text{Ca}^{2+}]_m$ accumulation can circumvent NADH oxidation due to elevated $[\text{Na}^+]_i$, 1 $\mu\text{mol/L}$ CGP-37157 was applied to the cells through the pipette to inhibit $[\text{Ca}^{2+}]_m$ efflux. With CGP-37157, the decay of $[\text{Ca}^{2+}]_m$ was slowed; the time to 50% decay of $[\text{Ca}^{2+}]_m$ increased by $34 \pm 11\%$ and $41 \pm 15\%$ in cells with 5 or 15 mmol/L Na^+ , respectively (half-times for $[\text{Ca}^{2+}]_m$ decay for all of the treatments studied are given in Supplementary Table S1). $[\text{Ca}^{2+}]_m$ accumulation during stimulation was enhanced in both groups (Figure 1E–F). Diastolic rhod-2 F/F0 in cells with 5 mmol/L $[\text{Na}^+]_i$ was 1.53 ± 0.09 at the end of stimulation and 1.30 ± 0.04 after 100 seconds recovery. This increase in $[\text{Ca}^{2+}]_m$ accumulation by CGP-37157 with 5 mmol/L $[\text{Na}^+]_i$ did not significantly change the NADH response to increased workload during stimulation (Figure 1G). Diastolic rhod-2 F/F0 in cells with 15 mmol/L $[\text{Na}^+]_i$ was 1.31 ± 0.06 at the end of stimulation and 1.25 ± 0.10 after 100 seconds recovery. Maintaining $[\text{Ca}^{2+}]_m$ accumulation by CGP-37157 abolished net NADH oxidation during pacing (Figure 1H; $64.8 \pm 6.3\%$ before stimulation; $62.3 \pm 6.0\%$ at the end of stimulation).

Effects of Inorganic Phosphate

P_i enhances $[\text{Ca}^{2+}]_m$ accumulation in isolated mitochondria, intact cells, and cardiac muscles^{11,12}; however, the effect of increased cytosolic P_i on $[\text{Ca}^{2+}]_m$ has never been directly demonstrated in isolated adult myocytes nor has its influence on metabolism been investigated. Therefore, we included 2 mmol/L K_2HPO_4 in the pipette solution to examine whether P_i can affect mitochondrial NADH production by enhancing Ca^{2+} accumulation. The most dramatic effect of P_i was to increase the duration of the $[\text{Ca}^{2+}]_m$ transient (Figure 2A–B). At the beginning of the 4-Hz stimulation, the time to 50% decay was increased by $58 \pm 21\%$ and $49 \pm 15\%$ in the cells with 5 and 15 mmol/L Na^+ , respectively, compared with controls (Figure 2A–B). This effect was even more pronounced when more Ca^{2+} accumulated in the matrix. At the end of stimulation, the plateau of the $[\text{Ca}^{2+}]_m$ transient was extremely elongated and by the end of our recording window for each pulse, peak $[\text{Ca}^{2+}]_m$ had decayed by only 30% to 40% (Figure 2C–D).

$[\text{Ca}^{2+}]_m$ accumulation during stimulation was enhanced by P_i . Diastolic rhod-2 F/F0 at the end of stimulation was 2.03 ± 0.20 and after 100 seconds recovery at rest was 1.31 ± 0.13 in cells with 5 mmol/L $[\text{Na}^+]_i$. With 15 mmol/L $[\text{Na}^+]_i$, diastolic rhod-2 F/F0 increased to 1.45 ± 0.06 with stimulation and was 1.24 ± 0.05 after 100 seconds rest (Figure 2E–2F). NADH level in cells with 15 mmol/L $[\text{Na}^+]_i$ was maintained during stimulation in the presence of P_i (NADH levels before and at the end of stimulation were $65.3 \pm 5.1\%$ and $63.6 \pm 3.0\%$, respectively; Figure 2H). Slight oscillations of NADH were noted in some cells treated with 2 mmol/L P_i during stimulation (Figure 2G–H).

We also examined an intermediate concentration of P_i (0.2 mmol/L) to determine if level that spans the physiological range gave similar results (Supplemental Figure S4). Again, an increase

in $[\text{Na}^+]_i$ from 5 to 15 mmol/L caused net NADH oxidation during stimulation, albeit with a longer delay and to a lesser extent than in the absence of added P_i . The relationship between $[\text{Ca}^{2+}]_m$ and NADH was essentially unchanged when these data were compared with the other interventions examined (see summary subsequently).

Effects of Ru360

Next we examined the effects of blocking mitochondrial Ca^{2+} uptake on the response to increased work. A total of 100 nmol/L Ru360 significantly inhibited $[\text{Ca}^{2+}]_m$ influx. On stimulation, a weak Ca^{2+} transient was still observed but with a slow rate of rise and smaller peak value (Figure 3E). Time-to-peak $[\text{Ca}^{2+}]_m$ with Ru360 was approximately 2-fold longer than controls, and the amplitude of the Ca^{2+} transient was only approximately 13% of that of controls. As a result, $[\text{Ca}^{2+}]_m$ accumulation during stimulation was decreased. At the end of stimulation, diastolic F/F0 of rhod-2 was 1.06 ± 0.01 and 1.06 ± 0.02 in cells with 5 and 15 mmol/L $[\text{Na}^+]_i$, respectively (Figure 3A–B). On stimulation, NADH fluorescence decreased monotonically in cells with either 5 or 15 $[\text{Na}^+]_i$ and did not recover after stimulation (Figure 3C–D), indicating that decreased $[\text{Ca}^{2+}]_m$ accumulation impaired mitochondrial NADH production. Compared with the levels before stimulation, NADH at the end of stimulation decreased by approximately 38% and approximately 43% in cells with 5 and 15 mmol/L $[\text{Na}^+]_i$, respectively.

Because 100 nmol/L Ru360 efficiently inhibited $[\text{Ca}^{2+}]_m$ influx, we further investigated whether the demonstrated effect of P_i on NADH production was secondary to its effect on $[\text{Ca}^{2+}]_m$ accumulation or if it had any effect on metabolism independent of $[\text{Ca}^{2+}]_m$. Myocytes were patch-clamped with a pipette solution containing 5 mmol/L Na^+ and Ru360 with or without 2 mmol/L P_i . On 4-Hz stimulation, NADH levels decreased similarly in cells with or without 2 mmol/L P_i in the pipette solution (Figure 3F).

NADH Redox Potential During Pacing in Myocytes From Failing Hearts: Effect of Enhancing $[\text{Ca}^{2+}]_m$ Accumulation

We have shown that elevated $[\text{Na}^+]_i$ impairs NADH supply during fast pacing by blunting the increase in $[\text{Ca}^{2+}]_m$, and this energy supply and demand mismatch can be prevented by enhancing $[\text{Ca}^{2+}]_m$ accumulation. To investigate whether impaired NADH production with elevated $[\text{Na}^+]_i$ is present in heart failure, and whether enhancement of $[\text{Ca}^{2+}]_m$ accumulation can improve energy balance, we established a guinea pig heart failure model by ascending aortic constriction based on a previously published model.^{11–14} At 6 to 8 weeks after surgery, heart weight, normalized to tibia length, was increased by approximately 85% and ejection fraction was decreased by approximately 20% when compared with age-matched controls (Table). In resting isolated cells that were not patch-clamped, $[\text{Na}^+]_i$ was elevated from 5.22 ± 1.36 mmol/L in control cardiomyocytes to 16.81 ± 3.13 mmol/L in the failing group (Table). To investigate whether the NADH/NAD⁺ balance was impaired during stimulation in myocytes from failing hearts, cardiomyocytes were field-stimulated at 4 Hz with 100 nM isoproterenol and NADH autofluorescence was recorded. In normal cardiomyocytes, NADH levels were maintained during 4-Hz stimulation (prestimulation: $51 \pm 3\%$; end stimulation: $54 \pm 3\%$; Figure 4A); however, in cardiomyocytes from failing hearts, NADH levels decreased dramatically during stimulation (prestimulation: $69 \pm 4\%$; end stimulation: $34 \pm 5\%$; Figure 4).

To test our hypothesis that $[\text{Ca}^{2+}]_m$ accumulation plays an essential role in maintaining NADH redox balance, myocytes from failing hearts were treated with CGP-37157 (10 $\mu\text{mol/L}$) added to the bath solution. The oxidation of the NADH pool in the failing group during 4-Hz field-stimulation was prevented by CGP-37157 treatment (pre-stimulation: $71 \pm 2\%$; end stimulation: $72 \pm 4\%$; Figure 4C).

We further investigated the role of elevated $[Na^+]_i$ in heart failure by fixing $[Na^+]_i$ in failing myocytes at 5 or 15 mmol/L using the patch clamp technique. When $[Na^+]_i$ of failing myocytes was maintained at 15 mmol/L, NADH level decreased during 4-Hz stimulation from $74\pm 3\%$ before stimulation to $45\pm 9\%$ at the end of stimulation (Figure 5C). In contrast, when $[Na^+]_i$ of failing myocytes was maintained at 5 mmol/L, the net oxidation of NADH during 4-Hz stimulation was largely eliminated (prestimulation: $77\pm 4\%$; end stimulation: $70\pm 4\%$; Figure 5D). Measurements of $[Ca^{2+}]_m$ indicated that decreased $[Na^+]_i$ (5 mmol/L) partially restored $[Ca^{2+}]_m$ accumulation in failing cells. At the end of stimulation, systolic and diastolic rhod-2 (F/F₀) in cells with 5 mmol/L $[Na^+]_i$ were 1.40 ± 0.02 and 1.29 ± 0.01 , respectively (Figure 5A). In contrast, in cells with 15 mmol/L $[Na^+]_i$, systolic and diastolic rhod-2 (F/F₀) were 1.26 ± 0.05 and 1.19 ± 0.03 , respectively (Figure 5B). Notably, $[Ca^{2+}]_m$ dynamics in failing cells were significantly different from normal cells (Figure 5E–H). The $[Ca^{2+}]_m$ transient in failing cells had a smaller amplitude and slower decay (Figure 5E–F), most likely the result of alterations in cytosolic Ca^{2+} handling associated with heart failure.

Threshold Level of Mitochondrial Ca^{2+} Required to Prevent Oxidation of the NADH Pool

To evaluate the effects of diastole or systolic $[Ca^{2+}]_m$ accumulation on NADH production, $[Ca^{2+}]_m$ at the end of stimulation was plotted against the decrease in NADH for the patch-clamp experiments described previously (Figure 6A–B). The results reveal that if $[Ca^{2+}]_m$ does not accumulate above a clear threshold level (F/F₀ approximately 1.31 for diastolic or approximately 1.45 for systolic) during pacing, there is an inverse linear correlation between $[Ca^{2+}]_m$ and the extent of NADH oxidation. Regardless of the specific intervention studied (eg, high $[Na^+]_i$, heart failure, Ru360), decreasing $[Ca^{2+}]_m$ increased the extent of NADH oxidation, whereas interventions that increase $[Ca^{2+}]_m$ loading (eg, CGP-37157, P_i, or lowering $[Na^+]_i$) abolished the net oxidation of NADH during stimulation. Below the threshold, $[Ca^{2+}]_m$ and NADH were highly correlated (diastolic $R=0.95$, $P<0.0001$; systolic $R=0.95$, $P<0.0003$), but the relationship was flat above the threshold. CGP-37157 or P_i was still able to enhance $[Ca^{2+}]_m$ significantly with 5 mmol/L $[Na^+]_i$, but no further effect on NADH balance was observed.

Discussion

The principal findings of the present study were: 1) the detrimental effect of elevated $[Na^+]_i$ on $[Ca^{2+}]_m$ accumulation and NADH production can be prevented by partial inhibition of the main $[Ca^{2+}]_m$ efflux pathway, mNCE, or by P_i, which enhanced mitochondrial Ca^{2+} uptake and prolonged the decay of the transient; 2) inhibition of mitochondrial Ca^{2+} uniporter blocks $[Ca^{2+}]_m$ accumulation, leading to net mitochondrial NADH oxidation at increased workload with either 5 or 15 mmol/L $[Na^+]_i$; 3) the kinetics of mitochondrial Ca^{2+} uptake are altered in myocytes from failing hearts, but are still dependent on $[Na^+]_i$; 4) increased resting $[Na^+]_i$ in heart failure contributes to impaired mitochondrial Ca^{2+} uptake during electric stimulation; and 5) the defective NADH response in heart failure can be reversed by enhancing mitochondrial Ca^{2+} uptake. Taken together, the results demonstrate that $[Ca^{2+}]_m$ plays a critical role in maintaining NADH redox potential during increased workload.

Mitochondrial Ca^{2+} Uptake

The present data and our previous work⁵ demonstrate that mitochondria take up Ca^{2+} rapidly with a time-to-peak value of approximately 20 ms and that a $[Ca^{2+}]_m$ transient is induced during each cytosolic Ca^{2+} transient (particularly when isoproterenol is present; Figure 1A). These results support a model of rapid mitochondrial Ca^{2+} uptake with a slow decay, resulting in accumulation of a sustained $[Ca^{2+}]_m$ signal. Although this subject is still controversial, a recent study by Bell et al¹⁵ came to a similar conclusion using mitochondrially targeted aequorin as

the Ca^{2+} sensor. Moreover, in that study, the $[\text{Ca}^{2+}]_m$ response to pacing was associated with an increase in mitochondrial matrix ATP measured using matrix-targeted luciferase.

In myocytes from failing hearts, the rise time of the $[\text{Ca}^{2+}]_m$ transient was reduced (Figure 5) and its amplitude was decreased with respect to controls. This is consistent with the known alterations in the kinetics of the cytosolic Ca^{2+} transient previously reported in this model.¹⁴ However, owing to the longer duration of the $[\text{Ca}^{2+}]_m$ transient in the failing group, the steady-state diastolic $[\text{Ca}^{2+}]_m$ at the end of stimulation was close to that of the controls (F/F0: 1.29 in failing versus 1.35 in controls). Furthermore, the suppressive effect of 15 mmol/L $[\text{Na}^+]_i$ on the diastolic $[\text{Ca}^{2+}]_m$ after 100 ms of pacing was similar to the control group (F/F0 1.19 in failing and 1.21 in controls) as was the NADH oxidation response. These findings suggest that the steady-state mitochondrial Ca^{2+} accumulation is more important for increasing NADH production than the size of the $[\text{Ca}^{2+}]_m$ transient during heartbeat consistent with the allosteric activation of TCA cycle enzymes, which would be expected to change more slowly to adjust to changes in metabolic demand.

An interesting, but as yet unexplained, finding was that increased $[\text{Na}^+]_i$, which tends to increase the amplitude of the cytosolic Ca^{2+} transient, not only slowed $[\text{Ca}^{2+}]_m$ decay, but also suppressed the amplitude of the $[\text{Ca}^{2+}]_m$ transient. This observation cannot be explained by increased efflux through mNCE or decreased influx through a possible reverse mode of mNCE because inhibition of mNCE by CGP-37157 did not restore the amplitude in high $[\text{Na}^+]_i$. A potential explanation for the effect of $[\text{Na}^+]_i$ could be that Na^+ could have a direct effect on mitochondrial Ca^{2+} uniporter activity. Although this explanation will require further investigation, a change in $[\text{Na}^+]_i$ is known to shift the apparent K_m for mitochondrial Ca^{2+} uptake in isolated mitochondria.¹

Mitochondrial Ca^{2+} Efflux

As the major Ca^{2+} efflux pathway in heart mitochondria, mNCE plays a key role in $[\text{Ca}^{2+}]_m$ handling. Compared with the rapid upstroke of the $[\text{Ca}^{2+}]_m$ transient, with a time-to-peak value of 20 to 30 ms, the time for decay of $[\text{Ca}^{2+}]_m$ from peak to diastolic levels takes more than 80 ms at the onset of stimulation with 5 mmol/L $[\text{Na}^+]_i$ (Figure 6G–6H; see Supplemental Table S1). In the absence of electric stimulation, mNCE balances mitochondrial Ca^{2+} efflux with influx, but when the amplitude and frequency of mitochondrial Ca^{2+} uptake is increased, the slower extrusion rate leads to matrix Ca^{2+} accumulation, which, as demonstrated here, is critical for maintaining NADH redox potential during increased work. The Na^+ dependence of mNCE explains why elevating $[\text{Na}^+]_i$ from 5 to 15 mmol/L increases the rate of $[\text{Ca}^{2+}]_m$ decay during the $[\text{Ca}^{2+}]_m$ transient (see Supplemental Table S1), blunts $[\text{Ca}^{2+}]_m$ accumulation during stimulation, and decreases $[\text{Ca}^{2+}]_m$ at the end of recovery.

An unexpected finding was that CGP-37157 treatment did not have a substantial effect on the initial slow decay of $[\text{Ca}^{2+}]_m$ on cessation of stimulation, although a somewhat higher offset of $[\text{Ca}^{2+}]_m$ was observed when mNCE was inhibited (see Figure 1E–F). With this in mind, additional experiments were performed to determine if the permeability transition pore might contribute as an alternative Ca^{2+} efflux pathway; however, these tests did not support a role for the PTP in mitochondrial Ca^{2+} efflux (Supplemental Figure S2).

Effects of Inorganic Phosphate

Mitochondria have high Ca^{2+} loading capacity, in part, because abundant P_i in the matrix forms a gel-like complex with Ca^{2+} , which is highly dynamic yet osmotically inactive.¹⁶ This Ca^{2+} and P_i complex provides a Ca^{2+} buffer system in the matrix that permits large increases in the total mitochondrial Ca^{2+} load.¹⁷ Enhancement of mitochondrial Ca^{2+} uptake by P_i has been demonstrated in isolated mitochondria,¹² intact muscles, and cardiac cells.¹⁸ In the

present study, we demonstrated that P_i increases $[Ca^{2+}]_m$ accumulation and maintains NADH production in cells with elevated $[Na^+]_i$. P_i markedly increased the duration of the $[Ca^{2+}]_m$ transient and was associated with a higher $[Ca^{2+}]_m$ at the end of recovery (Figure 3E–F). The Ca^{2+} buffering effect of P_i is not likely to explain the increased $[Ca^{2+}]_m$ transient amplitude, but may contribute to the prolongation of the decay kinetics, possibly facilitating retention of $[Ca^{2+}]_m$, because the matrix Ca^{2+} buffers load during fast pacing. On the other hand, more direct effects of P_i on the Ca^{2+} efflux or influx pathways are possible or an indirect effect on $\Delta\Psi_m$ or Na^+/H^+ exchange (through decreased ΔpH) could play a role. These alternative explanations will require further investigation.

In addition to effects on $[Ca^{2+}]_m$, P_i can also stimulate ATP synthesis through classical respiratory control¹⁹ as well as by relieving a block of electron transport at the level of cytochrome b,^{20,21} thereby promoting oxidation of NADH. Bose et al have also proposed that P_i activates TCA cycle dehydrogenases in parallel with activation of electron transport.²⁰ However, a contrary finding was recently reported by Jo et al,²² who demonstrated that P_i decreased NADH production in a dose-dependent manner, although this study was carried out in the absence of Ca^{2+} cycling in permeabilized myocytes. In our study, it is important to note that raising P_i in the cytoplasm did not alter the kinetics of net NADH oxidation when mitochondrial Ca^{2+} uptake was inhibited by Ru360 (Figure 3E). This provides compelling evidence that P_i does not activate the dehydrogenases independently of its effects on mitochondrial Ca^{2+} uptake in intact cells, arguing against a central role for P_i as a metabolic signaling molecule. The overall effect of P_i on energy supply and demand matching will reflect a competition between the multiple effects of P_i on Ca^{2+} accumulation, the TCA cycle, and respiration.

The Effects of Mitochondrial Ca^{2+} Accumulation on NADH Production

It is well documented that Ca^{2+} activates enzymes of TCA cycle and thus increases NADH production. In isolated mitochondria, Cox et al¹⁰ demonstrated that NADH level is dependent on extramitochondrial Na^+ concentration due to its effect on mitochondrial Ca^{2+} uptake, whereas we showed that elevated $[Na^+]_i$ blunts $[Ca^{2+}]_m$ accumulation and leads to a decrease in NADH during high-frequency stimulation in cardiomyocytes.⁵ In the present study, we show for the first time that this effect can be prevented by interventions that enhance mitochondrial Ca^{2+} uptake. The response of NADH changes in workload has been previously characterized by Brandes and Bers²³ using preloaded cardiac trabeculae. A rapid increase of work induced a transient decrease of NADH level followed by a nearly full recovery, and an abrupt decrease of work resulted in a transient overshoot of NADH. This NADH response was temporally correlated with changes in $[Ca^{2+}]_m$. However, studies in isolated cardiomyocytes have produced controversial results as to how NADH changes in response to a rapid increase of workload: an increase, decrease, or no change of NADH have all been reported.^{22,24,25} Based on the present findings, differences in resting $[Na^+]_i$ among cells²⁶ or between species⁶ could account for the variability in the NADH response in previous reports.

A technical consideration of the present methodology was that to calibrate the NADH signal in terms of percent reduction of the pool in individual cells, cyanide was applied at the end of each experiment to record the “100% reduced” state. This strategy tends to slightly overestimate the extent of NADH reduction in the basal resting state due to a decrease in the autofluorescence signal over time. Although the data were corrected for a linear bleaching rate, this problem could be exacerbated if there is additional (irreversible) oxidation of the NADH during fast pacing. This limitation would not substantially alter the conclusions of the study.

Our general findings revealed that at low $[Na^+]_i$, NADH levels are well compensated with no net change of NADH at the end of stimulation compared with the resting state. The response was distinctly different at 15 mmol/L $[Na^+]_i$ or when mitochondrial Ca^{2+} uptake was inhibited

with Ru360; net NADH oxidation occurred, monotonically and irreversibly. Thus, $[Ca^{2+}]_m$ plays an essential role in maintaining NADH production on increased workload in cells with elevated $[Na^+]_i$. The irreversibility of the NADH oxidation, despite the return of $[Ca^{2+}]_m$ to near resting levels, indicates that the metabolic state of the mitochondria changes if there is a mismatch between NADH production and respiration. This can be explained by an increase in oxidative stress on the myocyte during rapid pacing under high $[Na^+]_i$ (or Ru360) conditions, resulting in damage to components of oxidative phosphorylation. In separate experiments, we have documented increased mitochondrial reactive oxygen species production in the high $[Na^+]_i$ condition (data not shown); hence, an important message from this work is that the reducing environment of the mitochondrial matrix is crucial for maintaining the antioxidant capacity of the cell. This is manifested through the glutathione redox state, important for detoxifying hydrogen peroxide through peroxidase reactions, and through reduction of the thioredoxin and peroxiredoxin pools. These reactive thiol pools are maintained in the reduced state by NADPH,²⁷ kept in the reduced state in the matrix by 3 main reactions, 1) the NADH/NADPH transhydrogenase; 2) the malic enzyme; and 3) the NADP⁺-linked isocitrate dehydrogenase reaction.²⁷ The transhydrogenase reaction depends on the mitochondrial protonmotive force and NADH, whereas the latter 2 reactions depend on the levels of TCA cycle intermediates.

Remarkably, when $[Ca^{2+}]_m$ accumulation during work fell below a well-defined threshold, there was a linear inverse relationship between $[Ca^{2+}]_m$ and NADH. In cells with 15 mmol/L $[Na^+]_i$, application of CGP-37157 or P_i increased $[Ca^{2+}]_m$ above the threshold and the oxidation of NADH, and presumably the oxidative stress, was prevented. When $[Ca^{2+}]_m$ was above the threshold (eg, in 5 mmol/L $[Na^+]_i$ groups), although $[Ca^{2+}]_m$ could be markedly enhanced, no additional effects on NADH level during pacing were observed. This plateau effect of $[Ca^{2+}]_m$ on NADH was probably because the concentration of $[Ca^{2+}]_m$ was close to saturating with respect to the activation of the TCA cycle enzymes.

Role of Elevated $[Na^+]_i$ in Heart Failure

Studies of human cardiac muscles and animal models of cardiac hypertrophy and heart failure indicate that $[Na^+]_i$ is elevated from normal resting levels of 5 to 8 mmol/L up to 10 to 22 mmol/L.⁶⁻⁸ Elevated $[Na^+]_i$ in heart failure is thought to contribute a positive inotropic effect by enhancing cytosolic Ca^{2+} handling both by promoting the reverse-mode of NCX and by increasing the SR Ca^{2+} load (secondary to reduced Ca^{2+} extrusion through NCX). This is the rationale behind the therapeutic use of cardiac glycosides, which inhibit the sarcolemmal Na^+/K^+ ATPase. However, changes in the expression and activity of Ca^{2+} handling proteins (eg, increased NCX, decreased SERCA2A function, altered RyR activity) may offset these beneficial effects and contribute to arrhythmias.⁷ The present findings indicate that the effects of increased $[Na^+]_i$ on mitochondrial energetics and $[Ca^{2+}]_m$ are another negative factor that may compromise cardiomyocyte function in several ways. First, the impairment of mitochondrial Ca^{2+} loading could contribute to a loss of the normal local buffering effect of mitochondria near the dyad, which could contribute to uncontrolled spontaneous Ca^{2+} wave propagation. Second, the stimulation of NADH production by Ca^{2+} may be impaired, causing a mismatch in energy supply and demand. This effect would be exacerbated by the known defects in cytosolic Ca^{2+} handling in heart failure, which we reason are behind the slowed kinetics and more diminutive $[Ca^{2+}]_m$ transients in the failing group in the present study. Third, the net oxidation of the NAD(P)H pool could affect the antioxidant scavenging systems of the cell, particularly the ability to buffer reactive oxygen species produced by the mitochondrial respiratory chain. All of these actions could contribute to premature cell death in the context of chronic heart disease, which involves a sustained work overload condition, impaired Ca^{2+} handling, and extrinsic and intrinsic sources of oxidative stress.

The present findings demonstrate, for the first time, that the elevation of $[Na^+]_i$ in cardiomyocytes from failing hearts is correlated with impaired NADH responses to rapid stimulation with concomitant β -adrenergic activation. Importantly, the ability of the mNCE inhibitor to prevent the oxidation of the NADH pool immediately suggests a remedy for the negative effects of $[Na^+]_i$ in the context of either heart failure or cardiac glycoside toxicity while still preserving the potential positive inotropic effects of increased $[Na^+]_i$. The findings support our previous hypothesis that the combination of depressed Ca^{2+} cycling and elevated $[Na^+]_i$ in heart failure could lead to a vicious cycle of impaired adaptation to energy demand, net oxidation of the mitochondrial and cytoplasmic redox state and negative feedback on redox sensitive targets in excitation–contraction coupling.³ Elucidation of the both the feedforward and feedback effects of Ca^{2+} , Na^+ , and NAD(P)H redox balance on excitation–contraction–energetic coupling in normal and diseased hearts represents a fertile area of investigation in the future.

Supplementary Material

Refer to Web version on PubMed Central for supplementary material.

Acknowledgments

We acknowledge Dr Christoph Maack for his insightful discussions pertaining to the manuscript.

Sources of Funding

This work was supported by National Institutes of Health grants P01-HL081427 and R01-HL61711.

References

1. Denton RM, McCormack JG. Ca^{2+} as a second messenger within mitochondria of the heart and other tissues. *Annu Rev Physiol* 1990;52:451–466. [PubMed: 2184763]
2. Huser J, Blatter LA, Sheu SS. Mitochondrial calcium in heart cells: beat-to-beat oscillations or slow integration of cytosolic transients? *J Bioenerg Biomembr* 2000;32:27–33. [PubMed: 11768759]
3. Maack C, O'Rourke B. Excitation-contraction coupling and mitochondrial energetics. *Basic Res Cardiol* 2007;102:369–392. [PubMed: 17657400]
4. Gunter TE, Buntinas L, Sparagna G, Eliseev R, Gunter K. Mitochondrial calcium transport: mechanisms and functions. *Cell Calcium* 2000;28:285–296. [PubMed: 11115368]
5. Maack C, Cortassa S, Aon MA, Ganesan AN, Liu T, O'Rourke B. Elevated cytosolic Na^+ decreases mitochondrial Ca^{2+} uptake during excitation-contraction coupling and impairs energetic adaptation in cardiac myocytes. *Circ Res* 2006;99:172–182. [PubMed: 16778127]
6. Pieske B, Houser SR. $[Na^+]_i$ handling in the failing human heart. *Cardiovasc Res* 2003;57:874–886. [PubMed: 12650866]
7. Pogwizd SM, Sipido KR, Verdonck F, Bers DM. Intracellular Na^+ in animal models of hypertrophy and heart failure: contractile function and arrhythmogenesis. *Cardiovasc Res* 2003;57:887–896. [PubMed: 12650867]
8. Verdonck F, Volders PG, Vos MA, Sipido KR. Intracellular Na^+ and altered Na^+ transport mechanisms in cardiac hypertrophy and failure. *J Mol Cell Cardiol* 2003;35:5–25. [PubMed: 12623296]
9. Babsky A, Doliba N, Doliba N, Savchenko A, Wehrli S, Osbakken M. Na^+ effects on mitochondrial respiration and oxidative phosphorylation in diabetic hearts. *Exp Biol Med* 2001;226:543–551.
10. Cox DA, Matlib MA. A role for the mitochondrial Na^+ - Ca^{2+} exchanger in the regulation of oxidative phosphorylation in isolated heart mitochondria. *J Biol Chem* 1993;268:938–947. [PubMed: 8419373]
11. Langer GA, Nudd LM. Addition and kinetic characterization of mitochondrial calcium in myocardial tissue culture. *Am J Physiol* 1980;239:H769–H774. [PubMed: 7446751]

12. Lehninger AL. Role of phosphate and other proton-donating anions in respiration-coupled transport of Ca^{2+} by mitochondria. *Proc Natl Acad Sci U S A* 1974;71:1520–1524. [PubMed: 4364542]
13. Ahmmed GU, Dong PH, Song G, Ball NA, Xu Y, Walsh RA, Chiamvimonvat N. Changes in Ca^{2+} cycling proteins underlie cardiac action potential prolongation in a pressure-overloaded guinea pig model with cardiac hypertrophy and failure. *Circ Res* 2000;86:558–570. [PubMed: 10720418]
14. Siri FM, Krueger J, Nordin C, Ming Z, Aronson RS. Depressed intracellular calcium transients and contraction in myocytes from hypertrophied and failing guinea pig hearts. *Am J Physiol* 1991;261:H514–H530. [PubMed: 1831600]
15. Bell CJ, Bright NA, Rutter GA, Griffiths EJ. ATP regulation in adult rat cardiomyocytes: time resolved decoding of rapid mitochondrial calcium spiking imaged with targeted photoproteins. *J Biol Chem* 2006;281:28058–28067. [PubMed: 16882672]
16. Nicholls, DG.; Ferguson, SJ. *Bioenergetics 3*. Vol. 3rd ed.. London: Academic Press; 2002.
17. Chalmers S, Nicholls DG. The relationship between free and total calcium concentrations in the matrix of liver and brain mitochondria. *J Biol Chem* 2003;278:19062–19070. [PubMed: 12660243]
18. Ponce-Hornos JE, Langer GA, Nudd LM. Inorganic phosphate: its effects on Ca exchange and compartmentalization in cultured heart cells. *J Mol Cell Cardiol* 1982;14:41–51. [PubMed: 6278150]
19. Chance B, Williams GR. A simple and rapid assay of oxidative phosphorylation. *Nature* 1955;175:1120–1121. [PubMed: 14394122]
20. Bose S, French S, Evans FJ, Joubert F, Balaban RS. Metabolic network control of oxidative phosphorylation: multiple roles of inorganic phosphate. *J Biol Chem* 2003;278:39155–39165. [PubMed: 12871940]
21. Chance B. The energy-linked reaction of calcium with mitochondria. *J Biol Chem* 1965;240:2729–2748. [PubMed: 14304892]
22. Jo H, Noma A, Matsuoka S. Calcium-mediated coupling between mitochondrial substrate dehydrogenation and cardiac workload in single guinea-pig ventricular myocytes. *J Mol Cell Cardiol* 2006;40:394–404. [PubMed: 16480740]
23. Brandes R, Bers DM. Simultaneous measurements of mitochondrial NADH and Ca^{2+} during increased work in intact rat heart trabeculae. *Biophys J* 2002;83:587–604. [PubMed: 12124250]
24. Griffiths EJ, Wei SK, Haigney MC, Ocampo CJ, Stern MD, Silverman HS. Inhibition of mitochondrial calcium efflux by clonazepam in intact single rat cardiomyocytes and effects on NADH production. *Cell Calcium* 1997;21:321–329. [PubMed: 9160168]
25. White RL, Wittenberg BA. Effects of calcium on mitochondrial NAD(P)H in paced rat ventricular myocytes. *Biophys J* 1995;69:2790–2799. [PubMed: 8599685]
26. Diaz ME, Cook SJ, Chamunorwa JP, Trafford AW, Lancaster MK, O'Neill SC, Eisner DA. Variability of spontaneous Ca^{2+} release between different rat ventricular myocytes is correlated with Na^{+} - Ca^{2+} exchange and $[\text{Na}^{+}]_i$. *Circ Res* 1996;78:857–862. [PubMed: 8620606]
27. Vogel R, Wiesinger H, Hamprecht B, Dringen R. The regeneration of reduced glutathione in rat forebrain mitochondria identifies metabolic pathways providing the NADPH required. *Neurosci Lett* 1999;275:97–100. [PubMed: 10568508]

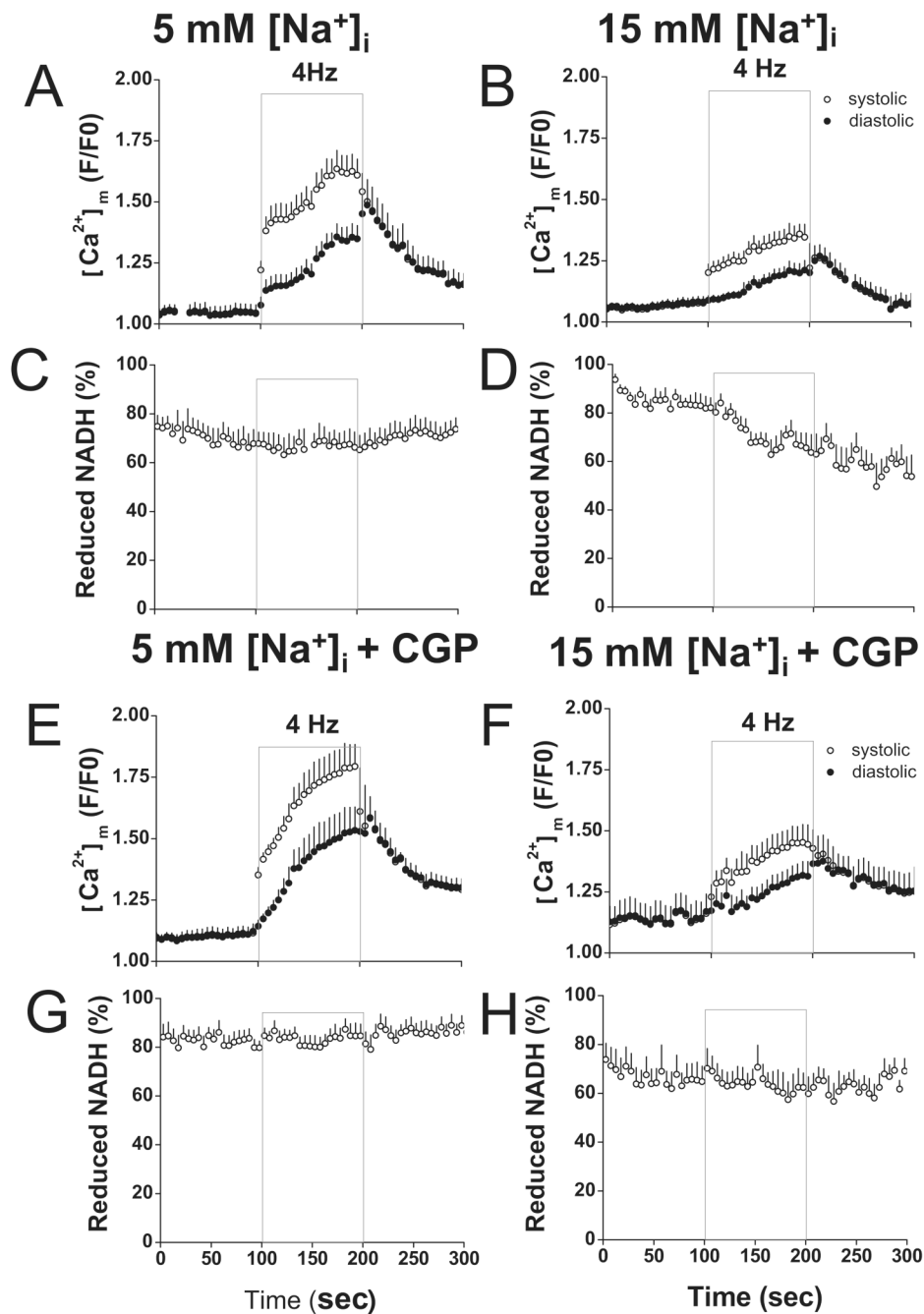
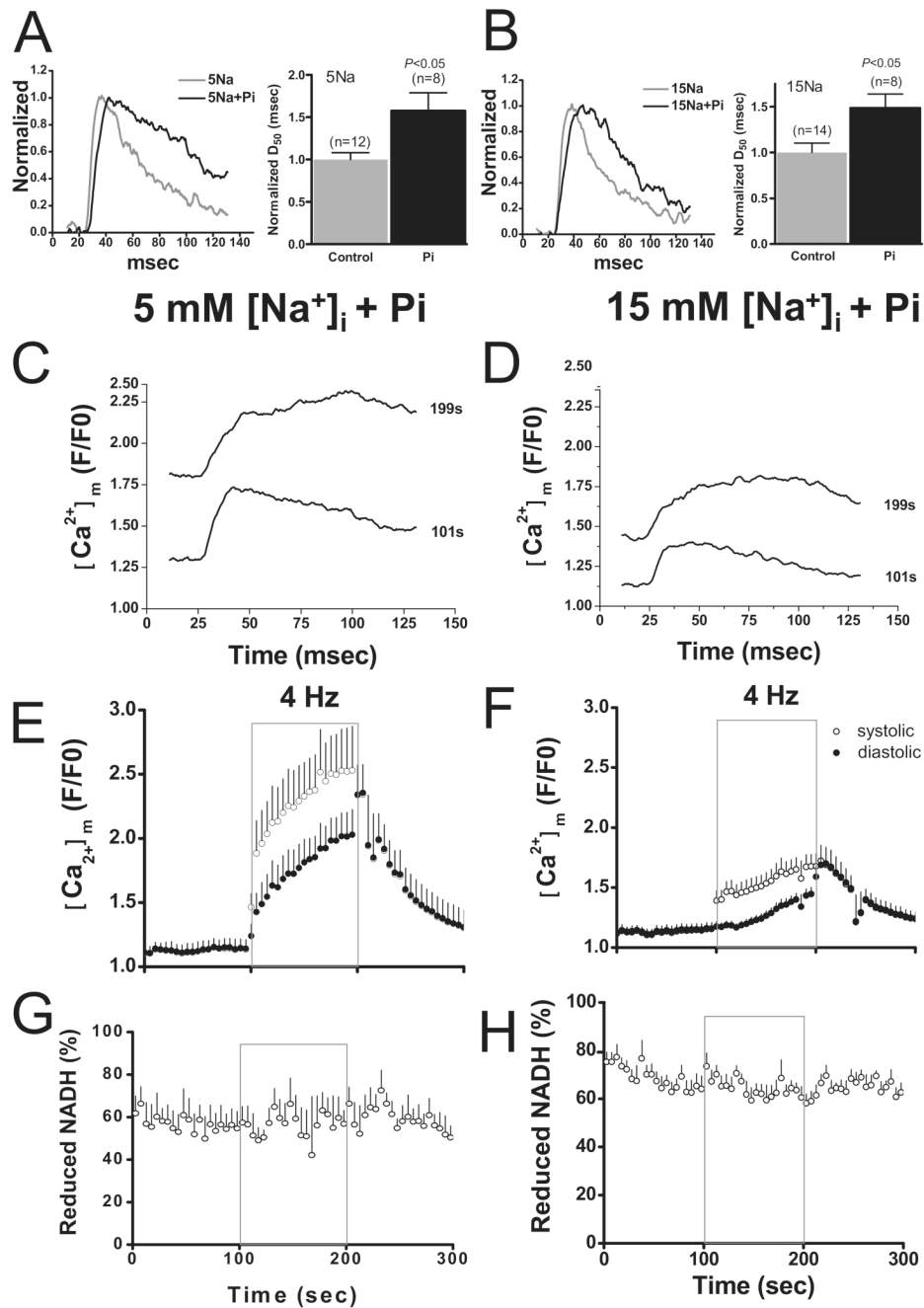


Figure 1. Effects of CGP-37157 on $[Ca^{2+}]_m$ accumulation and NADH production. Rhod-2 and NADH fluorescence were recorded simultaneously in patch-clamped myocytes with or without treatment of CGP-37157. In the presence of 100 nM isoproterenol, cells were recorded at rest, during 4-Hz stimulation (gray frame), and at rest again for recovery. Pipette solutions contained either 5 or 15 mmol/L Na^+ as indicated. A–D, Recording of rhod-2 and NADH without CGP-37157 in cells with 5 mmol/L Na^+ (A, C, n=11) and 15 Na^+ (B, D, n=14). E–H, Effects of treatment with CGP-37157 on rhod2 and NADH signals in cells with 5 mmol/L Na^+ (E, G, n=14) and 15 mmol/L Na^+ (F, H, n=8).

**Figure 2.**

Effects of P_i . A–B, Representative traces of $[Ca^{2+}]_m$ transients (left) and mean data of time to 50% decay (D_{50}) with or without 2 mmol/L P_i in cells with 5 (A) or 15 mmol/L Na^+ (B). C–D, Representative tracing of $[Ca^{2+}]_m$ transient recorded at the beginning (101 seconds) and the end (199 seconds) of stimulation with 5 (C) or 15 mmol/L Na^+ (D) in the presence of 2 mmol/L P_i . E–H, Recordings of rhod-2 (E–F) and NADH fluorescence (G–H) in cells with 5 or 15 mmol/L Na^+ .

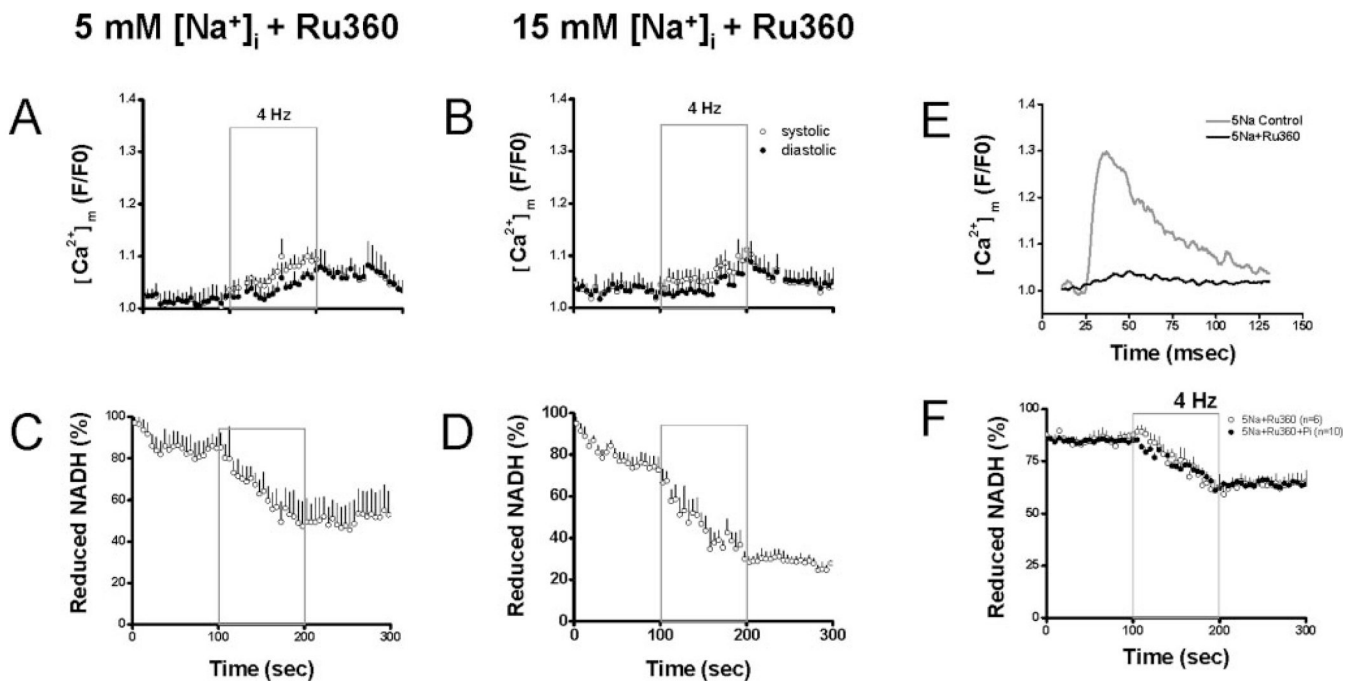


Figure 3.

Effects of Ru360. A–D, In the presence of Ru360, rhod-2 fluorescence (A–B) and NADH fluorescence (C–D) were recorded in cells with 5 or 15 Na^+ . E, Representative tracing of $[Ca^{2+}]_m$ transient with or without Ru360 in cells with 5 mmol/L Na^+ . F, Recording of NADH fluorescence in the presence of Ru360 alone or Ru360 plus P_i in cell with 5 mmol/L Na^+

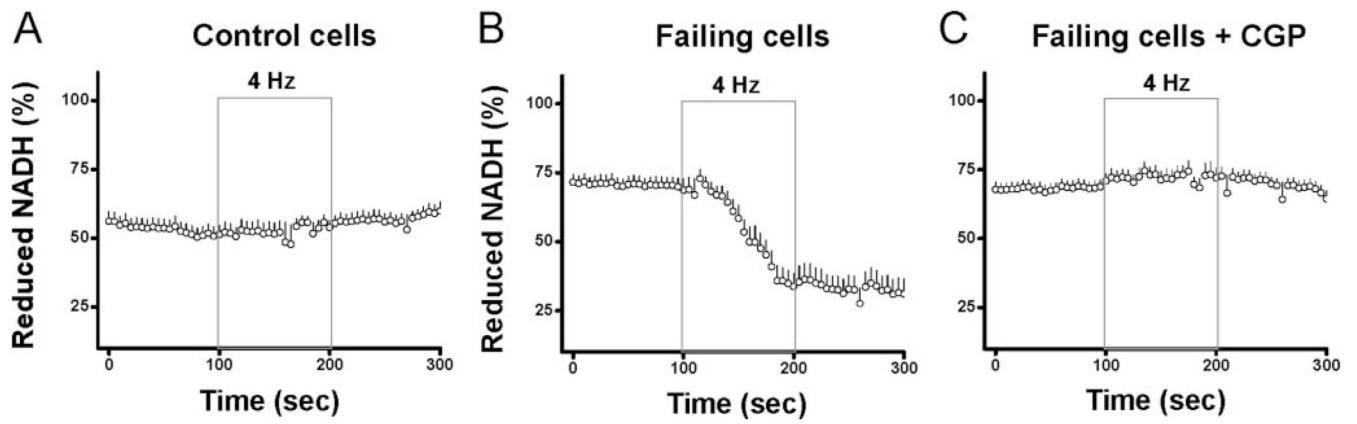


Figure 4.

Recording of NADH fluorescence in myocytes from control hearts (A, n=14) and failing hearts with (C, n=15) or without (B, n=19) CGP-37157. Cells were recorded at rest, during 4-Hz field stimulation, and on return to resting state.

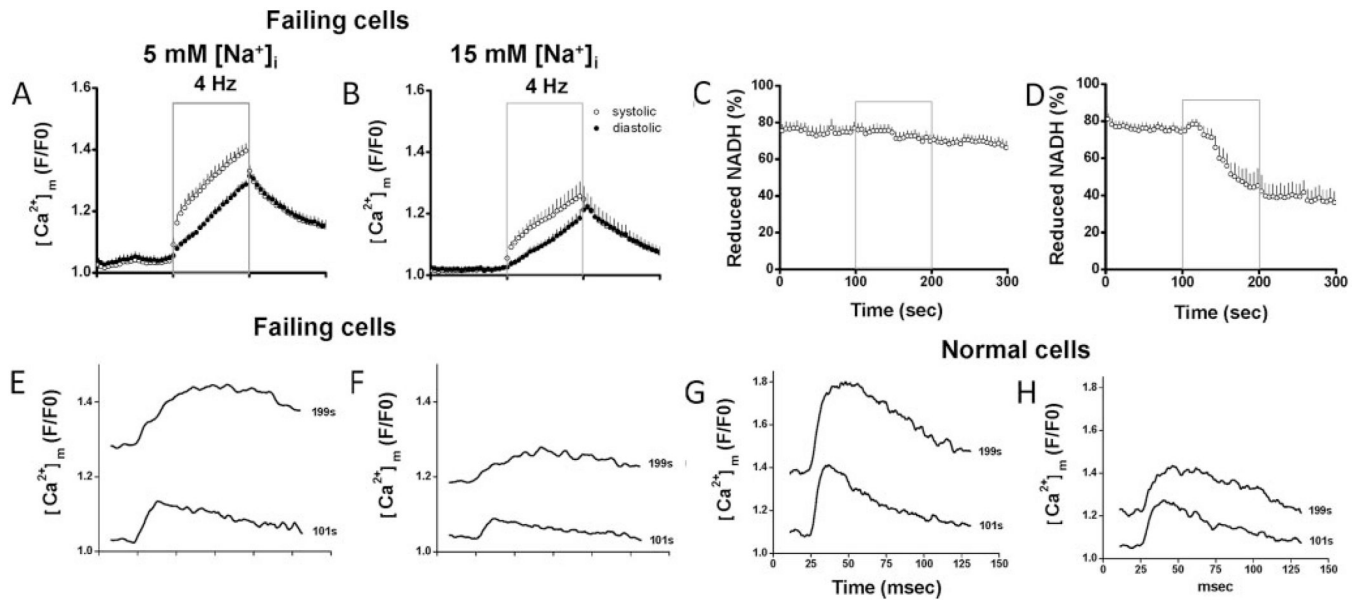


Figure 5.

Myocytes isolated from failing hearts were patch-clamped with pipette solutions containing either 5 (A, C, n=7) or 15 mmol/L (B, D, n=8) Na^+ . Recording of rhod-2 (A–B) and NADH fluorescence (C–D) are displayed. E–H, Representative tracing of $[Ca^{2+}]_m$ transient recorded at the beginning (101 seconds) or the end (199 seconds) of stimulation in cells from failing (E–F) and normal hearts (G–H) with 5 or 15 mmol/L Na^+

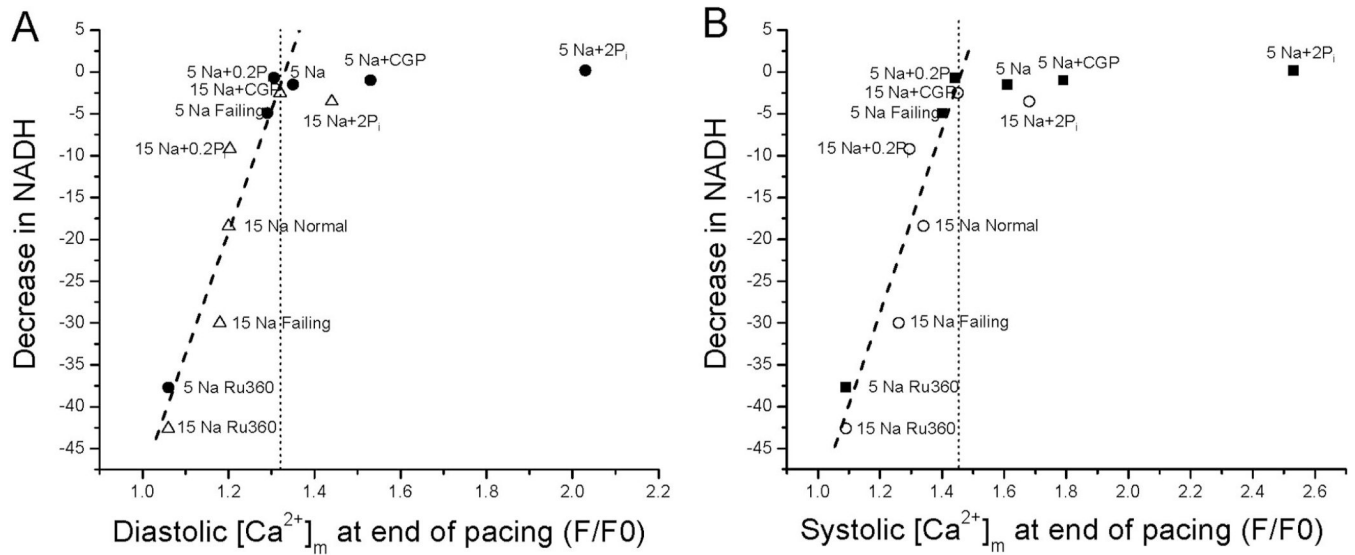


Figure 6. Threshold $[Ca^{2+}]_m$ required to prevent net NADH oxidation. Up to a threshold concentration of $[Ca^{2+}]_m$ (dotted lines in A–B), the extent of NADH oxidation at the end of the 100-second stimulation period was linearly correlated with $[Ca^{2+}]_m$ (A, diastolic rhod-2 F/F0; B, systolic rhod-2 F/F0). Beyond the threshold, further increases $[Ca^{2+}]_m$ did not alter the NADH balance. Filled and open symbols: 5 and 15 mmol/L Na^+ groups, respectively.

TableMeasurements of Heart Weight, Ejection Fraction, and $[\text{Na}^+]_i$

	No.	Heart Weight/Tibia Length, g/mm	Ejection Fraction, %	Na^+ Level, mmol/L
Control heart	4	0.50±0.04	62.0%±2.1	5.2±1.4
Failing heart	4	0.93±0.16*	49.8%±2.9*	16.8±3.1 [†]

* $P < 0.02$.[†] $P < 0.001$.